LEGIBILITY NOTICE

CONF-8705108--1

Los Alamos National Laboratory is operated by the University of California for the United States Department of Energy under contract W-7405-ENG-36

LA-UR--87-2126

DE87 011746

TITLE: PARITY NONCONSERVATION IN PROTON SCATTERING AT HIGHER ENERGIES

AUTHOR(S): R. E. MISCHKE
Los Alamos National Laboratory

SUBMITTED TO: Proceedings of the Symposium on Parity Non-conservation
TRIUMF, Vancouver, B. C., May 28-29, 1987

Los Alamos Los Alamos National Laboratory
Los Alamos, New Mexico 87545

PARITY NONCONSERVATION IN PROTON SCATTERING AT HIGHER ENERGIES*

R.E. Mischke
Los Alamos National Laboratory, Los Alamos, NM 87545

ABSTRACT

Parity-nonconservation experiments in the scattering of longitudinally-polarized protons at incident proton momenta of 1.5 GeV/c and 6 GeV/c are examined. These experiments indicate a change with energy of the total cross section correlated with proton helicity that was unexpected. This energy dependence is due to the strong part of the interaction and may indicate the role of a diquark component in the nucleon. New experiments at higher energies are needed to confirm such a model. Future experiments can benefit from an analysis of sources of systematic error that have been encountered in the experiments discussed here.

INTRODUCTION

The first experiments to search for parity nonconservation in proton scattering at higher energies used double-scattering[1] or triple-scattering[2] geometries. This technique was limited to a precision of ~10^{-3}. A new generation of experiments began in 1972 with a proposal to measure the helicity dependence of the transmission of 1.5 GeV/c longitudinally-polarized protons through an unpolarized target.[3] An interference between the strong amplitude and the parity-nonconserving weak amplitude is expected to produce a longitudinal asymmetry $A_L = (\sigma_+ - \sigma_-)/(\sigma_+ + \sigma_-)$ at the level of 10^{-7}, where $\sigma_+(\sigma_-)$ is the total cross section for positive (negative) helicity protons.

Since 1972 experiments have been performed at four energies. In each case several years have been required to reach the required level of precision. The experiment using a 15-MeV polarized beam at the Los Alamos Tandem Van de Graaff was begun in 1972 and ended about 1980. When a 6-GeV/c polarized beam became available at the Argonne ZGS, an experiment was started in 1974 and ended when the ZGS was closed in 1979. The 1.5-GeV/c experiment at LAMPF was begun in 1978 and completed in 1984. These experiments, together with experiments at 45 MeV sample the energy dependence of A_L. The group at SIN has continued to make improvements at 45 MeV and has just reported a measurement with unprecedented precision.[4]

A common theme of all these experiments is the identification and suppression of sources of systematic error. This paper will discuss the ZGS and LAMPF experiments in detail. The lessons learned from these experiments can be applied to future experiments at comparable or higher energies.

THEORETICAL AND EXPERIMENTAL BACKGROUND

When comparing experimental values of A_L with theoretical predictions, there is a contrast between the situation at low energies and at high energies. Measurements[5,4] of A_L at 15 and 45 MeV on

---

*Work supported by the U.S. Department of Energy.

hydrogen yield results of $A_L = (-1.7 \pm 0.8) \times 10^{-7}$ and $A_L = (-1.50 \pm 0.22) \times 10^{-7}$, respectively, in reasonable agreement with theoretical predictions based on a meson-exchange model[6-11] and a hybrid quark model.[12] (See Fig. 1.)

On the other hand, the experiment[13] with 6-GeV/c protons on a H_2O target has reported a value of $A_L = (26.5 \pm 6.0) \times 10^{-7}$, which is much larger than expected from calculations made prior to the experiment.[14,15] Later meson-exchange calculations[16,17] have confirmed the prediction of $A_L \sim 1.0 \times 10^{-7}$. Other theoretical approaches include the multi-peripheral model[18] and heavy boson exchange,[19] both of which also predict A_L to be $\sim 10^{-7}$. The contribution[20] from Coulomb effects is expected to give only a 15% enhancement of the asymmetry. A recent calculation used Regge theory to calculate the contribution to the asymmetry from parity nonconservation in the nucleon wave function.[21] The result is $A_L = +2.1 \times 10^{-6}$ with an estimated error of 30%, but this calculation has been criticized[22-25] because its extension to low energies yields predictions for several parity-nonconservation results that are much larger than the experimental values.

Most recently a calculation has been reported that considers the effects of parity nonconservation at the quark level. This calculation included both the scattering contribution and the wave-function part.[26,27] The wave functions were written in the SU(6) quark basis. The calculation was done as an operator product expansion and independently by writing amplitudes for one-loop graphs. Single-gluon exchange amplitudes were used for the strong interaction. The wave-function mixing effect is based on a sum of transitions to

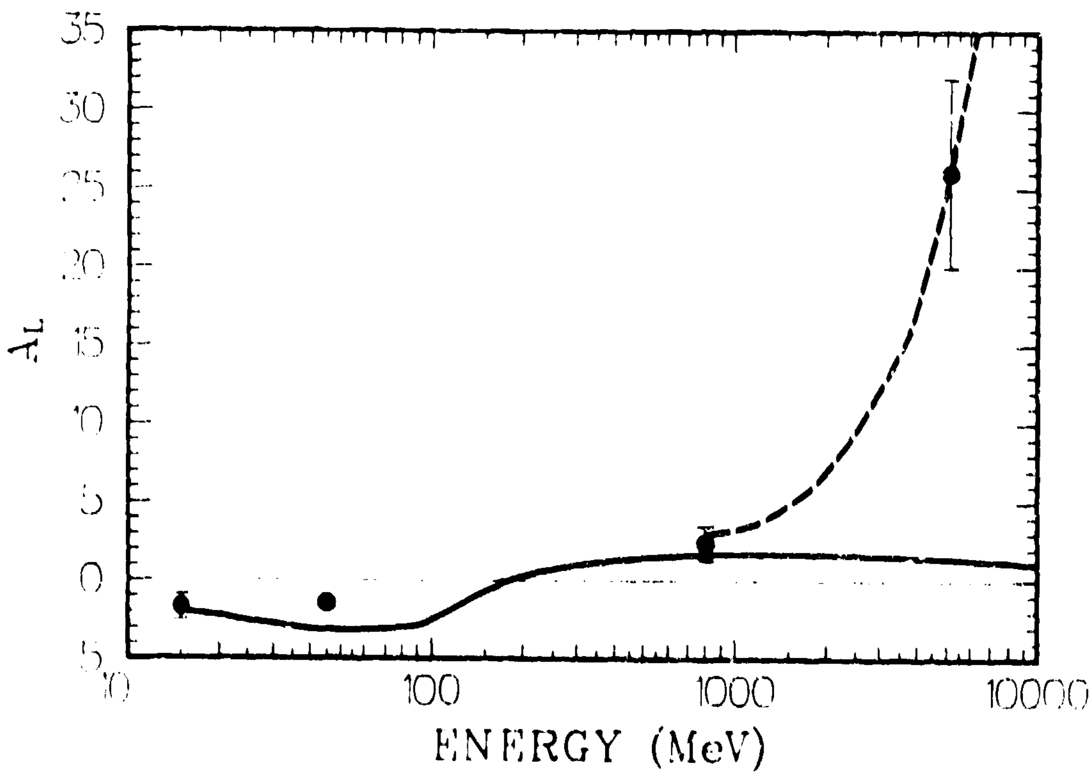

Fig. 1. Measured values of A_L versus energy. The solid curve is a generic meson-exchange calculation and the dashed curve is the model of Ref. 26.

negative-parity excited-nucleon states. The interaction takes place in the nucleon between one quark and a vector diquark. The results are dominated by the wave function part with $A_L = +(0.7 \text{ to } 2.7) \times 10^{-6}$. Although this model is expected to be valid only at high energy and the uncertainty is large, the result is very encouraging.

This and most other calculations have been for proton-proton scattering and have not considered nuclear effects and the role of the neutrons. A Glauber model calculation[28] predicts that the effect for p-p scattering should be a factor of 1.7 larger than that measured on water.

The experiments at 1.5 GeV/c (800 MeV) are at an energy intermediate to that of the previous measurements. Results have been published for polarized protons on an H_2O target[29] of $A_L = (1.7 \pm 3.3) \times 10^{-7}$ and $A_L = (2.4 \pm 1.1) \times 10^{-7}$ for an LH_2 target.[30] These results can be compared with a surprisingly large range of values among published predictions for the asymmetry at 1.5 GeV/c. The variation is mainly due to the use of different parametrizations of the strong nucleon-nucleon interaction. The predicted values for A_L from meson-exchange models range from (-8×10^{-7})[17] to $(+3 \times 10^{-7})$[16] with intermediate values of (-0.2×10^{-7})[31] and $(+2 \times 10^{-7})$.[14] A hybrid-quark model[12] predicts a value $\leq 1 \times 10^{-8}$, and the wave-function renormalization model[32],[33] predicts a large positive value $(+18 \times 10^{-7})$. If the high-energy quark-quark model[27] is extrapolated down to 1.5 GeV/c, the result is $+2 \times 10^{-7}$.

No theoretical approach describes the energy dependence of $\vec{p}$-nucleon scattering at all energies. The meson-exchange approach can explain experimental results at energies up to 1.5 GeV/c, but underestimates the 6-GeV/c result. The QCD approach is consistent with the 1.5- and 6-GeV/c results, but is not applicable at low energies. These experiments were originally envisioned as a study of the weak interaction between nucleons, but the most difficult parts of the problem for theorists are the strong-interaction aspects. The indication that the diquark component of the nucleon is important is very intriguing. An experiment at higher energy can confirm the energy dependence of A_L predicted by this model.

EXPERIMENTAL METHOD

The usual technique to determine A_L at higher energies is to measure the beam intensity before and after the target in a transmission geometry. An alternative is to monitor the incident or transmitted beam and detect scattered protons. At high energy the fractional asymmetry could be large enough to compensate for the reduced statistics in this geometry. If the detectors cover a large fraction of the angular range, measuring the integral of the scattered beam is equivalent to measuring the total cross section.

The ZGS experiment illustrates the transmission technique; the LAMPF experiments are similar. In the ZGS experiment, two independent detector systems measured the number of protons upstream and downstream of the target for each beam pulse. The detector currents were integrated, as the required beam intensities prohibited counting individual protons. The first detector system used scintillation counters. For this system, the transmission for one pulse of protons from the ZGS was measured as $Z_1 = T/I$ where T and I are the signals from the downstream and upstream counters, respectively. The second system used three identical ionization chambers. For each pulse, the signal from the downstream chamber D was subtracted from the upstream chamber, U, and normalized to the monitor chamber, M (located upstream). Thus $1 - Z_2 = (U - D)/M$.

Because each successive beam pulse had opposite helicity, the fractional change in transmission for each pair of pulses is $\zeta \equiv \Delta Z/2Z = (Z_+ - Z_-)/(Z_+ + Z_-)$ where $Z_+(Z_-)$ is the transmission (from either detector system) for the positive (negative) helicity pulse.

Fluctuations in ΔZ resulted from statistical uncertainties in the measurements of Z and from changes in Z due, for example, to random fluctuations in beam properties. The dependence of Z on beam motion and intensity fluctuations was removed by defining a corrected transmission, Z', for each pulse given by

$$Z' = Z - a_1(x-x_0)^2 - a_2(y-y_0)^2 - a_3(\langle i^2\rangle/I). \qquad (2)$$

Here $(x-x_0)$ and $(y-y_0)$ are horizontal and vertical deviations of the beam from the symmetry axis of the experiment (given by x_0, y_0). A measure of the time structure of the beam within a beam pulse is given by the square of the instantaneous beam intensity, $\langle i^2\rangle$, normalized to the beam intensity for the whole pulse, I. The dependence of Z on position is quadratic in lowest order because the beam was centered on a collimator and a displacement in any direction caused Z to decrease. The coefficients a_i were determined from a linear regression analysis to minimize fluctuations in Z'.

An average $\langle\zeta'\rangle$ was calculated for each run. The uncertainty in $\langle\zeta'\rangle$ was determined from rms fluctuations in ζ' and is designated $\delta\langle\zeta'\rangle$. Corrections were applied to the $\langle\zeta'\rangle$ from each run for known background processes such as residual transverse polarization that could give a change of transmission correlated with helicity, yielding

$$\langle\zeta'\rangle' = \langle\zeta'\rangle - \sum_i \gamma_i d_i \langle\Delta H_i\rangle \qquad (3)$$

where $\gamma(\mathrm{cm}^{-1})$ is the sensitivity constant for the term; d(cm) is the displacement of the beam from the symmetry axis; and $\langle\Delta H\rangle$ is the average change of a polarization-correlated quantity. The values of the H and d quantities were monitored each beam pulse and the γ values were measured in calibration runs.

An unanticipated source of asymmetry in the ZGS experiment was due to beam scattered by the small amount of material in those parts of the beam channel where the polarization was fully vertical. The scattered beam produced a signal in the I counter and U chamber that was correlated with beam helicity (to the extent that the beam was displaced from the effective center of the upstream detectors). In the runs measuring this so-called beam-matter interaction, the interaction probability was increased by adding a known amount of material in the channel and measuring the asymmetry.

After all runs were combined, a correction for the correlation between transverse polarization and position within the beam was applied to the weighted average. This last correction is given by $\gamma\varepsilon$ where γ is the sensitivity to transverse polarization and ε is the spatial first moment of the beam polarization distribution:

$$\varepsilon = \iint dx\, dy\, (xR_y(x,y) - yR_x(x,y))\, B(x,y) \ . \qquad (4)$$

x and y are particle coordinates at the collimator, $R_x(x,y)$ and $R_y(x,y)$ are the transverse polarization components for a given beam helicity, and B(x,y) represents the intensity distribution of the beam. It can be seen that a transverse component of polarization that averages to zero can produce a spurious parity signal.[5,34]

After all corrections have been applied, the value of $\langle\zeta'\rangle'$ is converted to the corresponding value of A_L.

ZGS EXPERIMENT

Polarized proton beam and target

The 6 GeV/c beam from the ZGS had an average intensity of 3.2×10^8 protons/pulse, a spill width of roughly 700 ms, and a repetition rate of 0.3 Hz. The polarization direction was reversed at the source each ZGS pulse. The polarization was vertical during acceleration in the synchrotron and remained so in the external proton beam.

A plan view of the beam line and apparatus is shown in Fig. 2. Most of the beamline was evacuated but the beam encountered the vacuum windows and air in some regions. A septum magnet separated the beam from the external proton beam. The magnet B2 deflected the beam upward through 7.75° to rotate the transverse polarization into the longitudinal direction.

Solenoids in the beam line were used to control the transverse polarization of the beam at the target. A quadrupole triplet focused the beam on the aperture of a brass collimator, C, located after the target. The spectrometer consisted of two bending magnets and four quadrupole magnets. Each bending magnet bent the beam downward and rotated the spin direction by 90° in the vertical plane. Quadrupoles focused the beam onto the transmission detectors.

The target was distilled water, enclosed in an aluminum cylindrical container. The container windows were made of flat quartz glass and were aligned parallel to each other and perpendicular to the incident beam direction. This design ensured that each beam particle encountered the same amount of material in the target. The transmission coefficient of the target was Z = 0.18 ± 0.01.

Detector systems

Most of the detectors were mounted on two rigid rails. Three scintillation counters were used for the transmission measurement. Each of these counters had a block of scintillator viewed by four photomultiplier tubes (PMT). The symmetrical arrangement of the PMTs

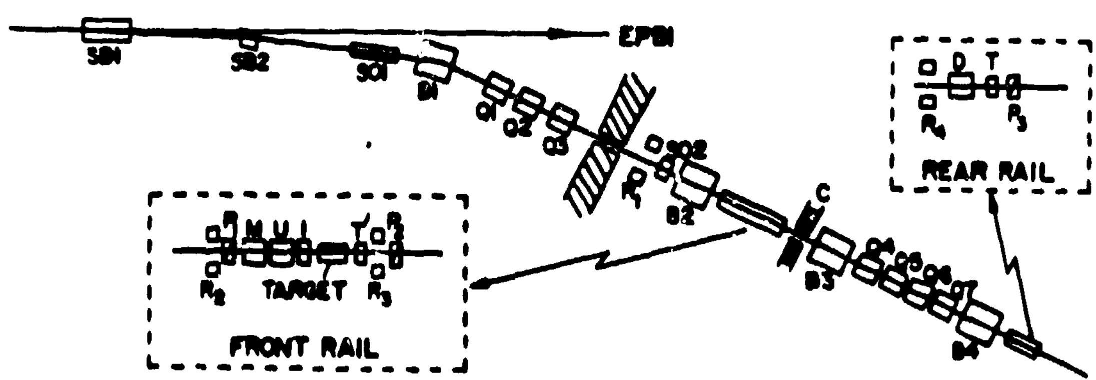

Fig. 2. Schematic diagram of the beam line and apparatus. Detectors and beamline components are described in the text.

about the beam direction helped to minimize the dependence of the summed signals on beam position. A fiber-optic cable, attached to each light guide, was used to inject a light pulse between each beam pulse for gain monitoring purposes. Counter I was located upstream of the target, T′ was just downstream of the target, and T was placed after the spectrometer.

Each of the three ionization chambers had 20 collector plates and 21 high-voltage plates. Each circular collector plate had guard rings on either side. A gas mixture of 90% argon and 10% methane was used in all three chambers. The operating pressure for the M and D chambers was ~40 psia and ~8 psia for U.

The beam position and polarization were measured every beam pulse by several sets of scintillation counters. The horizontal and vertical beam positions were measured by three sets of detectors with wedge-shaped scintillators, P_1, P_2, and P_3. Two complementary wedges, forming a block of scintillator, were optically isolated and connected to light guides and PMTs. Two such assemblies were mounted at right angles to each other and to the incident beam direction to form one position detector.

The R_1 and R_2 polarimeters measured the scattering asymmetries at the entrance to the experimental area due to material in the beam line. The R_3 detector monitored residual transverse polarization by measuring the left-right and up-down scattering asymmetry of the beam scattered from the water target. The R_4 detector monitored scattering in the magnetic spectrometer. Each detector consisted of four plastic scintillator counters with active regions located to the left, right, above, and below the beam line.

The beam centroid at position detector P_1 was stabilized pulse-to-pulse with the aid of a feedback loop. The voltage signals from the two horizontal PMTs of detector P_1 were used to control the current in magnet SB1. The time constant of the feedback loop, including the magnet response time, was ~100 ms.

The PMTs were selected to provide linear, noiseless gain with capability for a large dynamic range. Only five accelerating dynodes were used for the P_1, I, and T′ detectors, which were exposed to the full intensity of the beam. Detectors R_1, R_2, and R_4 used ten-stage PMTs. The current in each PMT was converted to a voltage by an operational amplifier and digitized by voltage-to-frequency converters (VTFs). The gain of each member of a group of detectors was matched to within 5%. The VTF output pulse train was scaled and recorded on magnetic tape each beam pulse.

Experimental procedure

The beam-line magnet currents were adjusted to maximize the transmission of the beam through the apparatus. Information from the calibration runs allowed the beam to be positioned on the null or symmetry axis of the experiment where contributions from beam-matter effects were minimized. The beam was focused at the collimator, the smallest aperture in the beamline, to minimize the noise due to beam motion. A transmission quality factor Q was defined as the ratio of measured fluctuations in the difference of transmission through the target for each helicity state to those fluctuations expected from statistical variations in the absorption process. By systematically adjusting the beam magnet currents, online Q-factors between two and seven could be attained, for both detector systems. The offline analysis could not remove these beam-induced transmission variations satisfactorily if the online Q-factors were larger than about ten.

There were 184 data runs with ~1600 pulses/run for a total of ~9×10^{13} protons on target. The rms variation of beam intensity was 4%. The rms resolution of the wedge detectors was about 15 μm. The pulse-to-pulse fluctuations of the beam position were 1 to 2 mm horizontally. In the vertical direction, beam motion was a factor of two smaller. Fast motion within a beam spill had amplitudes of up to ~5 mm and these were unaffected by the slow feedback. The difference in the beam position between positive and negative helicity protons as measured by P_1, averaged over all the data, was consistent with zero.

The polarimeters monitored scattering asymmetries throughout the experiment and the results are incorporated into the correction terms in Eq. (3). Averaged over all data runs, the residual vertical polarization was $(3.62 \pm 0.15) \times 10^{-4}$ and the horizontal polarization was $(-2.69 \pm 0.40) \times 10^{-4}$, compared to the longitudinal polarization of 0.71 ± 0.03 at the target. The average left-right scattering asymmetry measured by the R_2 detector is $(3.500 \pm 0.002) \times 10^{-3}$ due to material in the beam line.

Three types of calibration runs were taken to measure the sensitivity coefficients γ, for the correction terms in Eq. (3). A horizontal or vertical polarization of ~5% increased $\langle \Delta H \rangle = \langle \Delta R_{3x} \rangle$ or $\langle \Delta R_{3y} \rangle$ to $\sim 2.5 \times 10^{-3}$. Data were recorded with $\langle \Delta R_{3y} \rangle$ non-zero at increments of a few mm in $\langle P_{2x} \rangle$ and similarly at intervals of $\langle P_{2y} \rangle$ for $\langle \Delta R_{3x} \rangle$ non-zero.

Added-absorber runs to measure the beam-matter interaction effects were taken with 5 cm of Lucite placed about 2 m upstream from the center of B2, which increased $\langle \Delta R_{2y} \rangle$ by a factor of ten to $\sim 3.5 \times 10^{-2}$. The beam was moved a few mm left and right of beam center while the absorber intercepted the entire incident beam. Additional data were taken with Lucite absorbers of 1-cm and 2-cm thickness. By extrapolating the asymmetry from the data with Lucite to zero added absorber, the amount of scattering taking place during nominal data runs was determined to be equivalent to 5 mm of Lucite absorber.

Beam-partially-blocked runs to measure the polarization distribution in the beam were taken with either the top, bottom, left, or right half of the beam removed with a collimator.

Analysis and results

The signal from each phototube for each pulse was obtained by subtracting electronic offsets and dark current as measured in the appropriate gating intervals. The data selection procedure eliminated data from beam pulses with poor beam quality. The procedure used "quads" where a quad for variable X is defined as $X^q = X_i - X_{i+1} - X_{i+2} + X_{i+3}$, where pulse i has positive helicity. A quad has zero net polarization, an average value, $\langle X^q \rangle$, of zero, and is not affected by a linear gain drift during the four pulses. Acceptable quads had all beam pulses with more than 5×10^7 incident protons and no variables with negative offsets. The distribution of values of X^q is generally Gaussian and centered at zero but has enhanced tails. Because of these tails, the width of the distribution is defined as $\delta\langle X^q \rangle = 0.69(X^m)$ where X^m is the median of the absolute values of the quads. If X^q was greater than $2.5\ \delta\langle X^q \rangle$ for any of the six variables listed above, the data from the four beam pulses were rejected. These criteria removed about 10% of the data from each run.

A regression analysis was employed to reduce the effects of beam properties on the measured transmission. The evaluation of the coefficients in Eq. (2) was based on an analysis using the quad values of the variables. This made the results insensitive to any correlation between beam helicity and position or intensity. There is no evidence for a helicity correlation with these variables since each of the contributions is consistent with zero. The data from the R_1, R_2, and R_3 polarimeters were treated in a similar manner to remove position sensitivity in the polarization values.

The next stage of the analysis corrected for known helicity correlated quantities based on Eq. (3). The terms for residual transverse polarization mostly affected the T and D signals. The terms for beam-matter interaction mostly affected I and U. For each run, including calibration runs, the values of $\langle \zeta' \rangle$, $\langle \Delta R_i' \rangle$, and $\langle P_i \Delta R_i' \rangle$ were found. The coefficients were determined with a χ^2 minimization procedure applied to these values. The 10% of the runs that contribute a $\chi^2 > 5$ to the fit were rejected. The $\chi^2/\mathrm{df} = 1.17$ for both systems.

The result is $\langle \zeta' \rangle' = (-2.92 \pm 0.80) \times 10^{-6}$ for the scintillators and $\langle \zeta' \rangle' = (-4.96 \pm 0.93) \times 10^{-6}$ for the ion chambers. The correlation coefficient between values of $\langle \zeta' \rangle'$ for the two detector systems is 0.20 and was determined from the values for each run after all the corrections were made. The small value of this coefficient indicates that the measurements are essentially independent. A weighted average gives

$$\langle \zeta' \rangle' = (-3.73 \pm 0.62) \times 10^{-6} \quad . \tag{5}$$

For the final correction, the average helicity correlated components of polarization, $\langle \Delta R_y \rangle$ and $\langle \Delta R_x \rangle$, were measured with the beam partially blocked. Then $\varepsilon = a\gamma\,(\langle \Delta R_x \rangle - \langle \Delta R_y \rangle)$ where the coefficient a depends on the beam shape and the distribution of polarization across the beam. The polarization distribution arises from the process of extraction from the ZGS and from the effect of fringe fields in the magnetic transport of the beam. The known air and solid matter in the beam line broaden the beam size due to multiple scattering. Thus the beam profile is Gaussian and any higher-order components of the polarization distribution are washed out. As a result, a linear variation of polarization with position is expected with a Gaussian beam intensity shape, yielding $a = -\sqrt{2\pi}/8$. The value of γ is that determined for transverse polarization, leading to a correction of $(-0.50 \pm 0.37) \times 10^{-6}$ to $\langle \zeta' \rangle'$.

The parity-nonconservation asymmetry A_L is related to the net $\langle \zeta' \rangle'$, in the limit of small ΔZ, by the expression $A_L = 1/(|P| \ell n Z) \langle \zeta' \rangle'$. The result is

$$A_L = (2.65 \pm 0.60 \pm 0.36) \times 10^{-6} \quad . \tag{6}$$

The first error is statistical; it is dominated by the uncertainties in the individual measurements of the transmission that have been propagated through the analysis but also includes contributions from the statistical uncertainties in the corrections.

The second error is an estimate of systematic uncertainties. Because the largest correction to $\langle \zeta' \rangle$ comes from beam-matter interaction, several possible sources of error in the assumptions have been studied carefully. Data taken with the beam displaced 4 mm off the central axis yielded an unwanted 15% increase in the asymmetric halo measured at the I counter, due presumably to scattering from upstream apertures. However, the sensitivity of $\langle\zeta'\rangle$ versus position agrees with a linear dependence within statistics. In addition, placement of the Lucite scatterer along the beam line was studied and the position chosen was representative of the real distribution of matter. Finally, the introduction of additional scatterer upstream of the I counter did not change, within statistics, the asymmetric halo measured just downstream of the target. From these considerations a plausible systematic uncertainty is 20% of the correction, or 0.3×10^{-6}.

Another possible systematic error comes from uncertainties in the correction for the effect of polarization correlated with position within the beam. One contribution comes from a lack of direct knowledge of the shape of the polarization distribution across the beam profile. Another possible contribution is from the fact that the blocked-beam measurement was not taken at the location of the collimator. The total estimated uncertainty in the correction is 30%, leading to an estimated systematic uncertainty in the result of 0.2×10^{-6}. The measurement of this contribution was made near the end of the experiment; as a result there is no direct information on its stability with time. However, there is no evidence for drifts in the observed longitudinal asymmetry. If the observed asymmetry is the result of position-correlated polarization, this quantity must be large and constant during the long period of the data runs and then change abruptly to a small value at the point when it was measured. Such a change is very unlikely.

Other sources of systematic error, such as the treatment of residual transverse polarization and the effect of hyperon decay products, are negligible. From the energy dependence of the cross section and an upper limit on the correlation between beam momentum and helicity, this effect is estimated to be $< 2 \times 10^{-7}$. The effect of purely electronic sources of a false parity effect are tested by analyzing data taken with the beam off; the result is $A_L < 10^{-8}$. The result of analyzing the data grouped in a helicity suppressing pattern is $A_L = (0.5 \pm 0.6) \times 10^{-6}$. A test of drifts in the signals is an analysis of alternate runs starting with the opposite polarization; the results with this analysis are unchanged.

LAMPF EXPERIMENTS

The experiments performed at LAMPF utilized 1.5-GeV/c longitudinally polarized protons. A transverse magnetic field in the Lamb-shift-type ion source[35] reversed the proton helicity with a 30-Hz periodicity. The reversal frequency was chosen to be near a minimum in the spectral density of beam noise. The beam was accelerated to 800 MeV as H^- ions and reached the apparatus in macropulses of 500-μsec duration with a 120-Hz repetition rate. The beam intensity varied between 1 and 5 nA and the average polarization was $|P| = 0.70 \pm 0.03$.

The layout of the version of the experiment with a 1-m LH_2 target is presented in Fig. 3. The stripper foil was located 50 m upstream of the rest of the apparatus. An aperture in the foil defined the beam by stripping electrons from the H^- in the outer parts of the beam. The resulting H^+ were removed by a magnet. The transmission of protons through various targets was measured by two integrating ion chambers (I1 and I2), located upstream and downstream of the target. The statistical sensitivity of the measurement was limited by the available beam intensity as well as by detector noise due to nuclear spallation

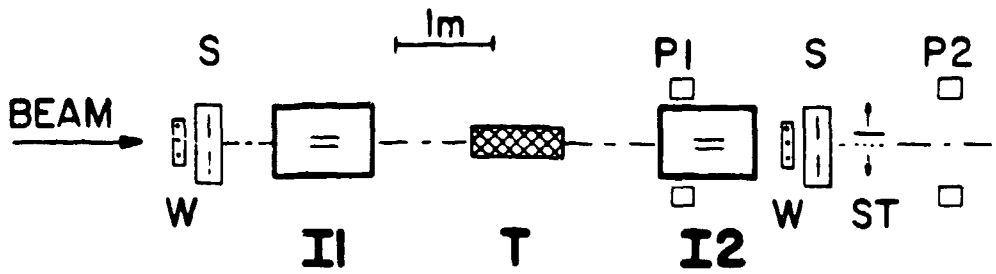

Fig. 3. Schematic of experimental setup. Detectors are described in the text.

reactions in ion-chamber surfaces. To reduce the second effect, spallation-minimizing ion chambers[36] were developed and used.

For the two helicity states of the beam, the fractional change in transmission was determined from the analog difference of the I1 and I2 signals. This difference signal was amplified before digitization to reduce round-off error. For each group of four pulses an analog to Eq. (1) was calculated. The helicity reversal pattern for the group of four pulses was + - - + to reduce the effects of drifts and to remove 60-Hz effects. At the end of a run, which consisted typically of 4×10^5 pulses, an average of ζ was calculated and a statistical uncertainty was computed from the fluctuations of ζ. For the 1-m LH_2 target the transmission was 0.85.

The beam position, intensity, size, and net transverse polarization (T_{pol}) were monitored for every pulse. In addition, the transverse-polarization distribution across the beam profile was sampled to determine ε.

Integrating multi-wire ion chambers,[37] W, monitored beam position and size for each pulse. Split-collector ion chambers, S, also monitored beam position and were part of a dual-loop feedback system that stabilized the average beam position and incident angle. A four-arm polarimeter, P1, used the LH_2 target s an analyzer to measure T_{pol} in the beam. A second polarimeter utilized a narrow target, ST, that continuously scanned the beam profile to measure ε. The upstream ion chamber of the transmission measurement recorded intensity variations of the incident beam.

To cancel contributions to A_L from beam changes uncorrelated to the beam helicity, the experiment was run for equal time periods in two different operating configurations (N and R) of the spin filter[35] in the polarized source. In both configurations protons exiting the source were longitudinally polarized, but positive helicity for the N and R configurations occurred during opposite phases of the spin-flip field of the source. The combination $(\zeta_N-\zeta_R)/2$ measures the longitudinal asymmetry while canceling some systematic effects and is referred to as the PNC signal. The combination $(\zeta_N+\zeta_R)/2$, called HIS, is expected to be zero and serves as a test for unidentified systematic errors.

To correct ζ for systematic contributions, its sensitivities to different systematics were determined. During the transmission measurement, each beam systematic was monitored. Final corrections to ζ were applied in the off-line analysis. Z values were corrected pulse-by-pulse for changes in beam intensity, position, and size. Corrections for T_{pol} were made for each group of four pulses, while corrections for ε and for unwanted electrical couplings were applied on a run-by-run basis. As a further test for unidentified systematic errors, the data were analyzed using a shift in the four-pulse grouping that eliminates any helicity dependence from the calculated A_L. The resultant value, A_L (shift), was consistent with zero.

The sensitivity of ζ to intensity modulations was determined using an apparatus[38] consisting of a set of stripper grids that were moved in and out of the H^- beam path to produce a 10% intensity modulation at 30 Hz. Stripper-grid data were taken as the DC intensity and size of the beam were varied. An analysis of these runs indicates a dependence: $d\zeta/dI = A_0 + A_1 I + A_2 I^2 + A_3/\sigma_x + A_4\sigma_y/\sigma_x$, where I is the beam intensity, $\sigma_x(\sigma_y)$ is the horizontal(vertical) width of the incoming beam, and the A_i are coefficients determined from the data. The terms containing I result from nonlinearities in the detectors and electronics. The size-dependent terms are consistent with recombination effects within the chambers.

During the experiment, contributions from polarization systematics were minimized by locating the beam along the symmetry-axis of the transmission detectors. To determine this axis, the transverse polarization was deliberately increased, and changes in ζ were measured as the beam was scanned across I1 and I2. The position servo-loop system held the beam on the symmetry axis. As a result, transverse polarization gives the smallest of all systematic corrections: a correction to A_L of $< 1 \times 10^{-8}$.

At each transmission detector, position scans were performed to measure the sensitivity of Z to position. The largest measured sensitivity was $dZ/dy = 1.3 \times 10^{-4}$/mm for vertical motion at the downstream detector. Small corrections for size variations were calculated from the quadratic components in the position dependence of Z. For approximately one third of all the runs the beam spot fell mostly on only two wires of the beam size monitor, and hence the beam size could not be accurately determined. Size corrections were not applied for these runs. In the runs where size corrections were applied, their contribution to A_L was negligible.

Any 30-Hz electrical pickup was kept out of the difference signal in two ways. First, a 15-Hz digital signal was used to transmit the helicity-reversal information from the polarized source to the experiment. Second, optical or analog isolators were inserted in all important signal paths. Residual pickup contributions were measured in runs taken with the beam off.

Applying the corrections improves the consistency of the data in several ways. First, within each run, corrected data have decreased pulse-to-pulse fluctuations in A_L because the correlations between ζ and various beam systematics have been removed by the application of the corrections. Second, when the data from all runs are tested for the hypothesis that HIS = 0 and that PNC has a definite value, the χ^2 value for the corrected data is nearly a factor of 2 smaller than χ^2 for the uncorrected data. The corrected HIS result is consistent with zero. The measured parity-nonconserving longitudinal asymmetry is $A_L = (+2.4 \pm 1.1 \pm 0.1) \times 10^{-7}$.

DISCUSSION

In both the LAMPF and ZGS experiments, each version of the experiment benefited from the earlier ones. The experience gained from these experiments may also be applied to future experiments. Most immediately this applies to the experiment underway at 230 MeV at TRIUMF. Other possibilities for future experiments include Saclay at 3 GeV, BNL at energies up to 22 GeV, and Fermilab at 200 GeV or higher.

The first measurement[39] at the ZGS found $A_L = (5.0 \pm 9.0) \times 10^{-6}$ using a Be target. It was found that the dominant contribution to the fluctuations in the measurements of Z was due to nonuniformities in the target coupled with random motion of the beam. This lead to the use of a water target with flat and parallel end windows in subsequent runs to ensure a uniform length and density for the target.

In the second version of this experiment,[40] A_L was found to be $(-15.0 \pm 2.4) \times 10^{-6}$. This value of A_L was attributed to the production of polarized hyperons in the target. Specifically, in the decay $\Lambda^0 \rightarrow p\pi^-$, the protons emerge preferentially along the direction of the lambda polarization and the pions preferentially against. The proton has an angular distribution peaked more forward in the laboratory frame than the pion. As the beam helicity is reversed, the angular distribution of the decay products is modified, which gives rise to a helicity-correlated signal. A collimator was inserted downstream of the center of the target that transmitted only 10% of the protons and 1% of the pions from lambda decay and less than 0.5% of the lambdas. In addition, a focusing magnetic spectrometer was installed to transmit only particles with the beam momentum minus the momentum loss in the target. This eliminated the decay products of the polarized hyperons produced in the target and therefore removed the spurious parity signal that could be caused by hyperon decay products striking the transmission detectors. A study[40] of the decay distribution of polarized lambdas with a Monte Carlo computer program, in which the longitudinal polarization transfer to the lambdas was assumed to be (0.26 ± 0.18), produced a cross section asymmetry $A_L = (31 \pm 23) \times 10^{-6}$. The result of the final experiment[41] using the T' detector, which reproduces the geometry of the detectors without the spectrometer, does not confirm the large negative asymmetry for the value of A_L but finds $A_L(T') = (3.9 \pm 0.72) \times 10^{-6}$ after all corrections.

The third experiment[42] included the spectrometer to eliminate hyperon decay products. A large transverse scattering asymmetry due to the beam-matter interaction was discovered (six times greater than the present experiment). The result was $(-26.3 \pm 7.5) \times 10^{-6}$. Since the existence of the beam-matter interaction was not realized until the end of the third experiment, the data from the second experiment were not corrected for beam-matter interaction, nor was there an attempt to position the beam on the symmetry axis. Thus it is probable that beam-matter interaction was responsible for the large negative result in the second and third versions.

In the final version the contribution from beam-matter interaction was reduced by evacuating the beam line where possible, adding helium elsewhere, and enlarging the aperture at the entrance to the experimental area just upstream of B2. Even so, the largest systematic correction to A_L in this experiment comes from the beam-matter interaction. The correction to A_L, with the beam carefully positioned on the symmetry axis, is -1.2×10^{-6}. Transporting a longitudinally polarized beam to the experimental area would eliminate this contribution to A_L. Otherwise beam halo can be a very subtle and time-dependent source of systematic error.

An attractive feature of the ZGS experiment was the ability to make two simultaneous independent measurements of A_L. Two detector systems with different properties increase the confidence in the final result by aiding in the understanding of systematic and random backgrounds. This experiment measured A_L with an accuracy of better than 6×10^{-7} in about a six-week period of data taking. The error is roughly three times greater than expected from the statistical fluctuations of the beam absorption in the target (Q-factor ~3).

With beam intensities above 5×10^8 protons/pulse, the Q-factor increased rapidly, precluding a more precise measurement of A_L in a reasonable amount of time with these detectors. The extra fluctuations in the transmission measurement in each detector system are uncorrelated and therefore did not originate from a common source. The dominant source of noise for the ion chambers was due to spallation in the plates.[36] Beam motion during the spill, 60 Hz and greater, contributed to the noise for the scintillation counters. To improve the Q-factor, a regression analysis removing beam motion from the transmission and a data-selection procedure, during the spill, could be accomplished by electronically dividing the beam spill into small time segments. The gain drifts of both detector systems were random and negligible.

Ion chambers perform well in intense beams but scintillation counters do not because of radiation damage to the plastic scintillator. The use of liquid scintillator instead of plastic scintillator is a possible solution to this problem. Alternatively, an experiment that measures only the scattered beam from the target with scintillation counters and the transmitted beam with ion chambers could utilize high beam intensities.

Early versions of the LAMPF experiment were plagued by high noise in the system. This was eventually traced to spallation in the ion chambers and lead to the design of new chambers. Next data were taken with an H_2O target. Control data were taken with a Pb target and no target as a check on the validity of the corrections and a test that other beam properties do not contribute to the PNC signal. The ideal control target would have all the properties of H_2O except the PNC contribution. The thickness of the Pb target was chosen to give the same amount of multiple Coulomb scattering as the H_2O target but with a factor-of-ten fewer nuclear interactions. Both the Pb and target-out measurements are less than ideal as controls because of reduced sensitivity to beam polarization effects due to low analyzing power, sensitivity to intensity that is different from H_2O, and statistical uncertainties about twice that of H_2O. The net corrected value of A_L for H_2O is $(1.7 \pm 3.3 \pm 1.4) \times 10^{-7}$.

The credibility of such experiments depends on the identification and study of all sources of systematic error greater than approximately half of the desired statistical accuracy. This is no easy task as there is no global test to determine the presence of a systematic contribution to A_L. Therefore, careful consideration should be given to detector systems that monitor beam properties and the models used to make corrections should be experimentally tested. Also, classes of systematics may be studied with unpolarized beam. The ZGS experiment had only a simple reversal of spin between pulses. A reversal pattern of +--+ can remove linear drifts. In addition there should be a method of reversing the proton spin external to the source. This helps to separate spin related systematics from those due to other beam properties. The LAMPF experiment included data with both helicities relative to the reversal signal.

The method used in these experiments to measure residual transverse polarization contributions to A_L could be repeated in a more sensitive measurement of A_L. A position feedback loop controlling the current in an upstream bending magnet is necessary to minimize beam motion and maintain the beam position on the symmetry axis to minimize effects of residual transverse polarization. The correlation of polarization with phase space should be measured at apertures that intercept scattered beam and can be determined by passing a thin scatterer through the beam and measuring the resulting transverse scattering asymmetry.[43]

Calibration runs should be repeated frequently during the experiment to compensate for changing conditions. In spite of the similarities of the sources of systematic error in the experiments described here, each accelerator is different and has its own potential for surprise.

CONCLUSIONS

The existing measurements of A_L at 1.5 GeV/c and 6 GeV/c indicate a strong energy dependence of the amplitude for the interference between the strong and non-leptonic weak interactions. New measurements at higher energies are needed to confirm this energy dependence and validate the quark-model predictions. These experiments are very difficult, but with adequate beam intensity and quality, the lessons of previous experiments should guide new efforts to a successful conclusion.

ACKNOWLEDGMENTS

My colleagues on the LAMPF and ZGS experiments are listed as the authors of Refs. 13 and 30. I am indebted to them and to the others listed in these references for the success of these experiments.

REFERENCES

1. E. J. Gucker and E. H. Thorndike, Phys. Rev. D 4, 2642 (1971).
2. P. Limon, L. Pondrom, S. Olsen, P. Kloeppel, R. Handler, and S. C. Wright, Phys. Rev. 169, 1026 (1968).
3. H. Frauenfelder, R. E. Mischke, and D. E. Nagle, spokesmen, LAMPF Proposal 137, 1972 (unpublished).
4. S. Kistryn, J. Lang, J. Liechti, Th. Maier, F. Nessi-Tedaldi, M. Simonius, J. Smyrski, S. Jaccard, W. Haeberli, and J. Sromicki, Phys. Rev. Lett. 58, 1616 (1987); R. Balzer et al., Phys. Rev. C 30, 1409 (1984).
5. D. E. Nagle et al., in High Energy Physics with Polarized Beams and Targets, edited by G. H. Thomas, AIP Conference Proceedings No. 51 (American Institute of Physics, New York, 1978), p. 224.
6. V. R. Brown, E. M. Henley, F. R. Krejs, Phys. Rev. Lett. 30, 770 (1973); Phys. Rev. C 9, 935 (1974).
7. M. Simonius, Phys. Lett. 41B, 415 (1972); Nucl. Phys. A220, 269 (1974).
8. Y. Yamamoto, Prog. Theo. Phys. 58, 1790 (1977).
9. G. N. Epstein, Phys. Lett. 55B, 249 (1975).
10. B. H. J. McKellar and K. R. Lassey, Phys. Rev. C 17, 842 (1978).
11. B. Desplanques, J. F. Donoghue, and B. R. Holstein, Ann. Phys. 124, 449 (1980).
12. L. S. Kisslinger and G. A. Miller, Phys. Rev. C 27, 1602 (1983).
13. N. Lockyer, T. A. Romanowski, J. D. Bowman, C. M. Hoffman, R. E. Mischke, D. E. Nagle, J. M. Potter, R. L. Talaga,

E. C. Swallow, D. M. Alde, D. R. Moffett, and J. Zyskind, Phys. Rev. D 30, 860 (1984).
14. E. M. Henley and F. R. Krejs, Phys. Rev. D, 11, 605 (1975).
15. V. B. Kopeliovich and L. L. Frankfurt, Pis'ma Zh. Eksp. Yeor. Fiz. 22, 601 (1975) [JETP Lett. 22, 295 (1975)].
16. T. Oka, Prog. Theo. Phys. 66, 977 (1981).
17. A. Barroso and D. Tadić, Nucl. Phys. A364, 194 (1981).
18. L. L. Frankfurt and M. I. Strikman, Phys. Lett. 107B, 99 (1981).
19. J. Soffer, in High-Energy Physics with Polarized Beams and Targets, edited by C. Joseph and J. Soffer, Experientia Supplementum Vol. 38, (Birkhäuser Verlag, Basel, 1981) p. 370; P. Chiappetta, J. Soffer, and T. T. Wu, J. Phys. G 8, L93 (1982).
20. A. S. Goldhaber, Phys. Rev. D 25, 715 (1982).
21. G. Nardulli and G. Preparata, Phys. Lett. 117B, 445 (1982).
22. J. F. Donoghue and B. R. Holstein, Phys. Lett. 125B, 509 (1983).
23. G. Nardulli and G. Preparata, Phys. Lett. 137B, 111 (1984).
24. B. H. J. McKellar, Phys. Lett. 138B, 6 (1984).
25. B. Desplanques and S. Noguera, Phys. Lett. 144B, 225 (1984).
26. T. Goldman and D. Preston, Nucl. Phys. B217, 61 (1983).
27. T. Goldman and D. Preston, Phys. Lett. 168B, 415 (1986)
28. L. L. Frankfurt and M. I. Strickman, Phys. Rev. D 33, 293 (1986).
29. R. W. Harper et al., Phys. Rev. D 35, 1151 (1985)
30. V. Yuan, H. Frauenfelder, R. W. Harper, J. D. Bowman, R. Carlini, D. W. MacArthur, R. E. Mischke, D. E. Nagle, R. L. Talaga, and A. B. McDonald, Phys. Rev. Lett. 57, 1680 (1986).
31. S. K. Singh and I. Ahmad, Phys. Letters 143B, 10 (1984).
32. G. Nardulli, E. Scrimeri, and J. Soffer, Z. Phys. C 16, 259 (1983).
33. G. Nardulli and G. Preparata, Phys. Lett. 137B, 111 (1984)
34. M. Simonius et al., Nucl. Instr. and Meth. 177, 471 (1980).
35. J. McKibben, in Polarization Phenomena in Nuclear Physics, edited by G. G. Ohlsen et al., AIP Conference Proceedings No. 69, (American Institute of Physics, New York, 1980), p. 830.
36. J. D. Bowman, R. Carlini, R. Damjanovich, R. E. Mischke, D. E. Nagle, R. L. Talaga, R. W. Harper, and V. Yuan, Nucl. Instr. and Meth. 216, 399 (1983).
37. D. W. MacArthur, R. E. Mischke, and J. P. Sandoval, Nucl. Instr. and Meth. A245, 262 (1986).
38. D. W. MacArthur, Nucl. Instr. and Meth. A243, 281 (1986).
39. J. D. Bowman, C. M. Hoffman, C. F. Hwang, R. E. Mischke, D. E. Nagle, J. M. Potter, D. M. Alde, P. G. Debrunner, H. Frauenfelder, L. B. Sorensen, H. L. Anderson, and R. Talaga, Phys. Rev. Lett. 34, 1184 (1975).
40. R. L. Talaga, Ph.D. dissertation, University of Chicago, 1976 (unpublished).
41. N. S. Lockyer, Ph.D. dissertation, Ohio State University, 1980 (unpublished).
42. D. M. Alde, Ph.D. dissertation, University of Illinois, 1978 (unpublished).
43. W. Haeberli, R. Hennick, Ch. Jacquemart, J. Lang, R. Müller, M. Simonius, W. Reichart, and Ch. Weddigen, Nucl. Instr. and Meth. 163, 403 (1979).